Walking Patterns and Actuator Specifications for a Biped Robot

Qiang HUANG, Shuuji KAJITA, Noriho KOYACHI, Kenji KANEKO, Kazuhito YOKOI

Tetsuo KOTOKU, Hirohiko ARAI, Kiyoshi KOMORIYA, and Kazuo TANIE

Department of Robotics, Mechanical Engineering Laboratory
1-2 Namiki, Tsukuba, Ibaraki, 305-8564 Japan
E-mail: {huang, kajita, koyachi, kaneko, yokoi, kotoku, harai, kiyoshi, tanie}@mel.go.jp

Abstract

Since most conventional robots cannot easily be adapted to environments designed for humans, a human-size biped robot is expected to be able to play an important role in assisting human activities. The selection of suitable joint actuators is an important point when developing a human-size biped robot. In order to select suitable actuators and effectively utilize the selected actuators, it is necessary to clarify the relationship between walking patterns and the specifications of each joint actuator, and this is the issue tackled in this paper. First, a method of generating a high stability, smooth walking pattern is presented, and it is shown how various walking patterns can be produced by setting a series of defined walking parameters. Then, the dynamics of the robot, including the reaction force between the feet and the ground, are formulated. Finally, by simulation studies, the correlation found between actuator specifications and walking patterns is described, and the effectiveness of the proposed method is suggested.

1. Introduction

In an increasingly elderly society, the need for utilizing robots to assist with human activities has grown rapidly. Since wheeled robots cannot be easily adapted to environments designed for humans, humanlike biped walking robots are expected to play an important role in such areas. Many interesting studies on biped robots have been reported [1-20].

One main topic in biped robot research is the generation of a walking pattern. This topic is mainly studied from two angles. One is to generate a minimum-energy gait. For example, McGeer [1] described a natural walking pattern generated by passive interaction of gravity and inertia on a downhill slope; Channon, et al. [2], Rostami, et al. [3], Roussel, et al. [4], and Chevallereau, et al. [5] have studied gait generation on level ground and uphill slopes by minimizing the cost function of energy consumption; and Silva, et al. [6] have proposed a method for minimizing the actuator power by adjusting walking parameters. The other approach is to synthesize a high stability walking pattern. For example, Zheng, et al. [7] have proposed a method of gait synthesis considering static stability; Takanishi et al.

[8], Shin et al. [9], Hirose et al. [10], Huang et al. [11] have proposed methods of walking pattern synthesis based on the ZMP (Zero Moment Point) [12] to realize dynamic walking for a biped robot.

It is important to consider minimum-energy when generating walking patterns, but the above-mentioned previous investigations only discuss the minimum of the total power or energy of all joint actuators. Actually, walking patterns also correlate strongly with the specifications of each joint actuator separately. We can observe human locomotion to explain this viewpoint. The pelvis and the trunk are held almost upright during the locomotion of a person without disability, but are often seen to be not upright during the locomotion of a person with a hip joint disability (Fig. 1). The incline of the pelvis and trunk is due to the lack of hip muscle strength [14, 15]. In addition, we can imagine our self-locomotion when some joint is sprained or some muscle is in pain. In such a case, our walking patterns are different from normal. Why do we choose such an abnormal walking pattern when disabled or injured? The reason must be that this abnormal walking pattern only requires a small amount of muscle strength from the injured joint, which cannot provide the performance necessary for normal walking.

It is possible to ignore the restrictions of actuator specifications if each joint has a large power actuator. But in this case, the robot size, weight, and the energy consumption become crucial issues, particularly in developing a human-size biped robot or humanoid robot [16].
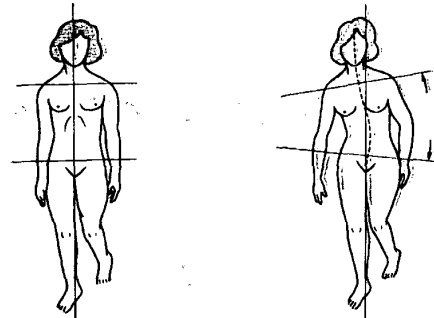
(a) Normal locomotion: the pelvis and trunk are upright.

(b) Abnormal locomotion: the pelvis and trunk incline

Fig. 1 Human locomotion [15]

In this paper, the objective is to clarify the relationship between walking patterns and actuation specifications, and the paper is organized as follows. In section 2, a high stability, smooth walking pattern is generated by a 3rd order spline function, and we show that various walking patterns can be obtained by setting the constraint values of walking parameters. The dynamics of the robot, including the reaction force between the feet and the ground are analyzed in section 3, and the correlation between actuator specifications and walking patterns is discussed with simulation results in section 4. Finally, a conclusion is given in section 5.

2. Walking Pattern

We consider a planar seven-link biped robot with a trunk (Fig. 2). Each leg consists of a thigh, a shin and a foot, and actuated hip, knee, and ankle joints.

A complete walking cycle is composed of a double-support phase and a single-support phase. During the double-support phase, both feet are in contact with the ground. This phase begins with the heel of the forward foot touching the ground, and ends with the toe of the rear foot taking off the ground. During the single-support phase, while one foot is stationary on the ground and the other foot swings from the rear to the front.

If both foot trajectories and the hip trajectory are known, all joint trajectories of the biped robot will be determined by kinematic constraints. The walking pattern can therefore be denoted uniquely by both foot trajectories and the hip trajectory. For a sagittal plane, each foot trajectory can be denoted by a vector $\mathbf{X}_a = [x_a(t), z_a(t), \theta_a(t)]^T$, where $(x_a(t), z_a(t))$ is the coordinate of the ankle position, and $\theta_a(t)$ is the slope of the foot. The hip trajectory can be denoted by a vector $\mathbf{X}_h = [x_h(t), z_h(t), \theta_h(t)]^T$, where $(x_h(t), z_h(t))$ denotes the coordinate of the hip position, and $\theta_h(t)$ denotes the slope of the hip (Fig. 2).

To enable the robot to adapt to ground conditions, we first specify both foot trajectories, then determine the hip trajectory, as described below and in Fig. 3.
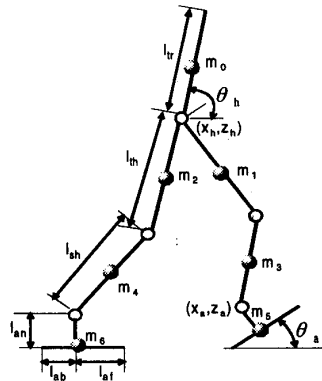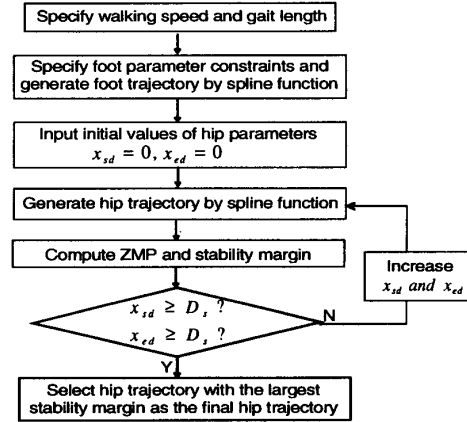

Fig. 2 Model of the biped robot

Fig. 3 Algorithm for planning walking patterns

2.1 Foot Trajectories

Supposing that the period necessary for one walking step is T_c, the time of the kth step is from kT_c to $(k+1)T_c$, $k = 1, 2, \cdots$. To simplify the analysis, we define the kth walking step to begin with the heel of the right foot leaving the ground at $t = kT_c$, and end with the heel of the right foot touching the ground at $t = (k+1)T_c$. In the following, we discuss only the generation of the right foot trajectory. The left foot trajectory is same as the right foot trajectory except for a T_c delay.

Let q_b and q_f be the designated slope angles of the right foot as it leaves and lands on the ground (Fig. 4) respectively. Since the whole sole of the right foot is in contact with the ground at $t = kT_c$ and $t = (k+1)T_c + T_d$, the characteristic constraints of the right foot slope are given by the following equations:

$$
\theta_a(t) = \begin{cases}
q_s(k) & t = kT_c \\
q_b & t = kT_c + T_d \\
q_f & t = kT_c + T_c \\
q_e(k) & t = (k+1)T_c + T_d
\end{cases} \tag{1}
$$

where T_d denotes the time interval of the double-support phase, and $q_s(k)$ and $q_e(k)$ are the slopes of the ground surface at contact points, in particular $q_s(k) = q_e(k) = 0$ on level ground.

Let (L_{ao}, H_{ao}) be the coordinate of the highest point of the swing foot (Fig. 4). From the kinematic constraints, the characteristic constraints of the right foot position are given as follows:

$$
x_a(t) = \begin{cases}
kD_s & t = kT_c \\
kD_s + l_{af}(1 - \cos q_b) + l_{an}\sin q_b & t = kT_c + T_d \\
kD_s + L_{ao} & t = kT_c + T_o \\
(k+2)D_s - l_{ab}(1 - \cos q_f) - l_{an}\sin q_f & t = kT_c + T_c \\
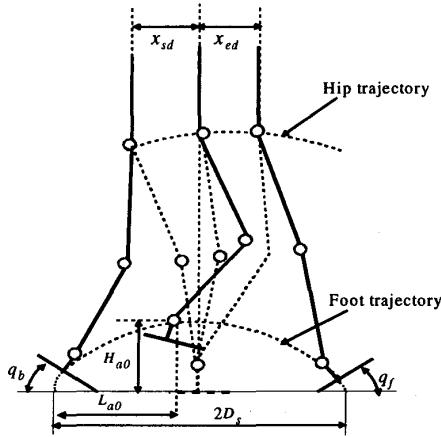(k+2)D_s & t = (k+1)T_c + T_d
\end{cases} \tag{2}
$$

Fig. 4 Parameters of walking pattern

$$z_a(t) = \begin{cases} l_{an} & t = kT_c \\ l_{an}\cos q_b + l_{af}\sin q_b & t = kT_c + T_d \\ H_{a0} & t = kT_c + T_o \\ l_{an}\cos q_f + l_{ab}\sin q_f & t = kT_c + T_c \\ l_{an} & t = (k+1)T_c + T_d \end{cases} \tag{3}$$

where $kT_c + t_o$ is the time when the right foot is at its highest point, D_s is the length of one step, l_{an} is the height of the foot, l_{af} is the length from the ankle joint to the toe, and l_{ab} is the length from the ankle joint to the heel (Fig. 2).

To generate a smooth trajectory, it is necessary that the second derivatives (accelerations) $\ddot{\theta}_a(t)$, $\ddot{x}_a(t)$ and $\ddot{z}_a(t)$ be continuous at all t, including all breakpoints $t = kT_c$, $kT_c + T_d$, $kT_c + T_o$, $(k+1)T_c$, $(k+1)T_c + T_d$.

If we solve for the foot trajectory which satisfies constraints (1), (2), (3) and the constraints of second derivative continuity by using polynomial interpolation, the order of the polynomial is too high. In this case, the computation of polynomial is difficult, and the trajectory may oscillate. Therefore, we obtain the foot trajectory by 3rd order spline interpolation (see Appendix A). In that case, $x_a(t)$, $z_a(t)$ and $\theta_a(t)$ are characterized by 3rd order polynomial expressions, and the second derivatives $\ddot{\theta}_a(t)$, $\ddot{x}_a(t)$ and $\ddot{z}_a(t)$ are always continuous. By setting the values of q_b, q_f, $q_s(k)$, $q_e(k)$, L_{ao}, H_{ao} and D_s, we can easily produce different foot trajectories.

2.2 Hip Trajectory

In theory, it is possible to produce different kinds of hip motion by adjusting $x_h(t)$, $z_h(t)$ and $\theta_h(t)$. However, since the biped robot tends to tip over easily, $\theta_h(t)$ and $x_h(t)$ should be mainly determined by stability constraints. Thus, only $z_h(t)$ can be designated arbitrarily within a fixed range.

Suppose the hip is at its highest position H_{hmax} at the middle of the single-support phase, and at its lowest position

H_{hmin} at the middle of the double-support phase; $z_h(t)$ has constraints given as follows:

$$z_h(t) = \begin{cases} H_{hmin} & t = kT_c + 0.5T_d \\ H_{hmax} & t = kT_c + 0.5(T_c - T_d) \\ H_{hmin} & t = (k+1)T_c + 0.5T_d \end{cases} \tag{4}$$

The trajectory of $z_h(t)$ that satisfies equation (4) and the second derivative continuity condition is obtained by 3rd spline interpolation.

From the viewpoint of stability, it is desirable that $\theta_h(t)$ is constant in the case that there is no waist joint; in particular, $\theta_h(t)=0.5\pi$ [rad] in the case of level ground. The change of $x_h(t)$ is a main factor affecting the stability for a biped robot walking in a sagittal plane. Some researchers [8,10] have proposed to derive $x_h(t)$ by using a desired ZMP (Zero Moment Point, Appendix B) trajectory. However, not all desired ZMP trajectories will be achieved [21], and the hip motion along x-axis may be too large even if the desired ZMP trajectory is achieved. In order to get a smooth hip motion along the x-axis with high stability, we take the following steps:

(1) Generate a series of smooth $x_h(t)$.

(2) Determine the final $x_h(t)$ with a large stability margin

$x_h(t)$ during a one-step cycle can be described by one function for the double-support phase and one function for the single-support phase. Letting x_{sd} and x_{ed} denote distances along the x-axis from the hip to the ankle of the stance foot at the beginning and the end of the single-support phase respectively (Fig. 4), we get the following equation:

$$x_h(t) = \begin{cases} (k+1)D_s - x_{sd} & t = kT_c + T_d \\ (k+1)D_s + x_{ed} & t = (k+1)T_c \\ (k+2)D_s - x_{sd} & t = (k+1)T_c + T_d \end{cases} \tag{5}$$

The initial constraints such as $x_h(t_0)=0$, and the final constraints such as $x_h(t_n)=0$, are known. By using 3rd order spline interpolation, we can obtain an $x_h(t)$ trajectory that satisfies constraints (5) and second derivative continuity. We get a series of smooth $x_h(t)$ by setting different values of x_{sd} and x_{ed} within fixed ranges, in particular $0 < x_{sd} < D_s$, $0 < x_{ed} < D_s$. Then, smooth trajectory $x_h(t)$ with the largest stability margin (see Appendix B) can be found by iterative computation (Fig. 3).

3. Dynamic Analysis

In order to simulate accurately the dynamic behavior of a biped robot, it is necessary to construct an accurate model of the robot and its interaction with environment. The ground reaction force between the feet and the ground strongly affects the behavior of the biped robot. For example, if the ground reaction force changes frequently, the biped robot will easily vibrate and become unstable; and if the ground reaction force is too large, the joint burden of supporting the robot will become large, and consequently

the torque and the power to drive joints increase.

The spring-damper element is usually used to model the normal force between the feet and the ground. Letting K_f and D_f be the stiffness coefficient and the damping coefficient, respectively, the ground normal force F_n is given as follows:

$$F_n = K_f \delta + D_f \dot{\delta} \qquad (6)$$

where δ is the penetration depth of the contact foot into the ground.

However the spring-damper model has some deficiencies [23-24]. One main defect is the ground normal force may be negative, because δ easily becomes negative just before the contact foot and the ground separate. A negative ground normal force implies that the ground pulls the contact foot, which is not correct physically in the case of usual ground. In order to obtain a suitable model of the ground reaction force, we introduce the Young's modulus - coefficient of restitution element [25] in the following.

Let E_m be the Young's modulus of the contacting materials, and C_r be the coefficient of restitution. If $C_r = 0$, the contact is perfectly inelastic; if $C_r = 1$, the contact is perfectly elastic. The ground normal force is given as follows:

$$F_n = \begin{cases} 0.733 E \sqrt{\frac{1}{r}} \left[1 + \left(\frac{1 - C_r^2}{1 + C_r^2} \right) \tanh\left(2.5 \frac{v_p}{v_t} \right) \right] \delta^{1.5} & |v_p| < |v_t| \\ 0.733 E \sqrt{\frac{1}{r}} \left[1 \pm 0.99 \left(\frac{1 - C_r^2}{1 + C_r^2} \right) \right] \delta^{1.5} & |v_p| = \pm|v_t| \\ 0.733 E \sqrt{\frac{1}{r}} \left[1 + \left(\frac{1 - C_r^2}{1 + C_r^2} \right) \right] \delta^{1.5} & |v_p| > |v_t| \end{cases} \qquad (7)$$

where v_p and v_t denote the penetration velocity and the transition velocity between the contact foot and the ground respectively, and r is the contact curvature. Then, the friction force F_f is given by the following equation:

$$F_f = \mu \tan(\frac{v_p}{v_t}) F_c \qquad (8)$$

where μ is the nominal friction coefficient. The motion equation of the biped robot is given as follows:

$$M(q)\ddot{q} + H(q,\dot{q}) = T + D(q)F \qquad (9)$$

where q is the vector of joint angles, $M(q)$ is the inertial
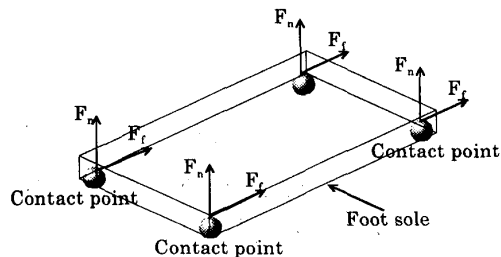
matrix, $H(q,\dot{q})$ is the vector of Coriolis, centrifugal, and gravitational terms, $D(q)$ is the kinematic constraints matrix depending on the location of contact points, T is the vector of actuator torque, and F is the vector of the ground reaction force including the normal force and the friction force (Fig. 5). The solutions of equation (9) can be obtained by published methods [26-28] or some commercial dynamic analysis software packages [29].

4. Simulation

We have constructed a simulator of a biped robot (Fig. 6) on an SGI workstation by using the dynamic software package DADS (Dynamic Analysis and Design System [29]). This allows us to easily analyze various factors such as the necessary joint torque, the ground reaction force between the feet and the ground. Parameters of the biped robot (Fig. 2) are set according to Table 1.

By specifying different values of H_{hmax}, H_{hmin}, H_{ao}, L_{ao}, q_b, q_f, $q_s(k)$, $q_e(k)$ and D_s, we can produce different walking patterns. In the following, we discuss the simulation in the case of 2.0 [km/h] speed walking ($D_s = 0.5$ [m], $T_c = 0.9$ [Sec]) on level ground ($q_s(k) = q_e(k) = 0$).

Fig. 7 shows the simulation results for different foot clearances H_{ao}. It is known that high foot clearance requires large maximal torque and velocity of almost all joints. This can be considered the reason that the higher the swing foot lifts, the larger the energy required to drive the joint is. Therefore, in order to minimize the specifications of joint actuators or energy consumption, it is desirable to have the biped robot walk without excessively lifting the swing foot.

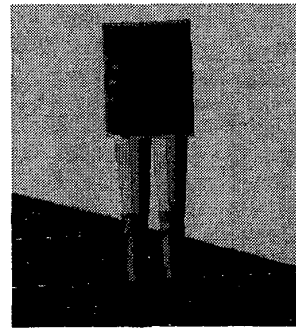The simulation results for different hip height H_{hmax}

Fig. 6 Biped robot in simulator

Table 1 Parameters of the biped robot

Length (cm)	l_{tr}	l_{th}	l_{sh}	l_{an}	l_{ab}	l_{af}
	60	40	40	10	10	13

Weight (kg)	m_0	m_1	m_2	m_3	m_4	m_5	m_6
	36	7.0	7.0	3.7	3.7	1.3	1.3

Inertia (kgm^2)	I_{0y}	I_{1y}	I_{2y}	I_{3y}	I_{4y}	I_{5y}	I_{6y}
	0.69	0.16	0.16	0.08	0.08	0.01	0.01

Fig. 5 Model of ground reaction force

1465

and H_{hmin} but same other parameters are shown in Fig. 8. The knee joint maximal torque in the case of a high hip position is less than the case of a low hip position (Fig. 8(b)), but other specifications are almost same. We can consider that this is because the robot needs to bend its knee joint more in the case of a low hip position, so large knee joint torque is required to support the robot. Therefore, from the viewpoint of reducing the burden on the knee joint, it is essential to keep the hip at a high position.

Fig 9 shows the simulation results for different foot slopes q_b. If the foot touches or leaves the ground as in $q_b = 0.0$ [rad] and $q_f = 0.0$ [rad] at the begin and end of the double-support phase, the hip cannot be held at a high position, and large maximal torque of knee joint is required (Fig. 9(b)). On the other hand, it is possible for the hip to be held at a high position by setting large values of q_b and q_f. But, in this case, since it is necessary to lift the heel of the rear foot to a sufficient height at the end of the double-support phase, the required maximal velocity of the knee joint increases (Fig. 9(d)(e)(f)), and consequently the required power of the joint increases.

5. Conclusion

Walking patterns correlate strongly with the actuator specifications of each joint. In this paper, in order to clarify the relationship between walking patterns and actuation specifications, first a method of generating a high stability, smooth walking pattern has been presented, and it was shown that various walking patterns can be obtained by setting the walking parameters. Then the dynamics, including the reaction force between the feet and the ground, were formulated, and the correlation between actuation specifications and walking patterns was provided by simulation results.

By using the proposed method, it is possible to obtain a walking pattern with small actuation specifications, select suitable actuators to realize a desired walking pattern, and determine a suitable speed reduction (using gears or pulley-belts) ratio for each joint.

Appendix A: 3rd Spline Interpolation

For n breakpoints $t_1 < t_2 < \cdots < t_n$, $S(t_j) = f_j$, $j = 1,2,\cdots,n$, the 3rd order spline function $S(t)$ is a 3rd order polynomial for each (t_j, t_{j+1}), and the first derivative $S'(t)$ and second derivative $S''(t)$ are continuous on (t_1, t_n).

Let $I_j = (t_j, t_{j+1})$, $h_j = t_{j+1} - t_j$, $S(t)$ is denoted by the following equation:

$$S(t) = \frac{M_j}{6h_j}(t_{j+1} - t)^3 + \frac{M_{j+1}}{6h_j}(t - t_j)^3 +$$

$$(f_j - \frac{M_j h_j^2}{6})\frac{t_{j+1} - t}{h_j} + (f_{j+1} - \frac{M_{j+1} h_j^2}{6})\frac{t - t_j}{h_j} \qquad (10)$$
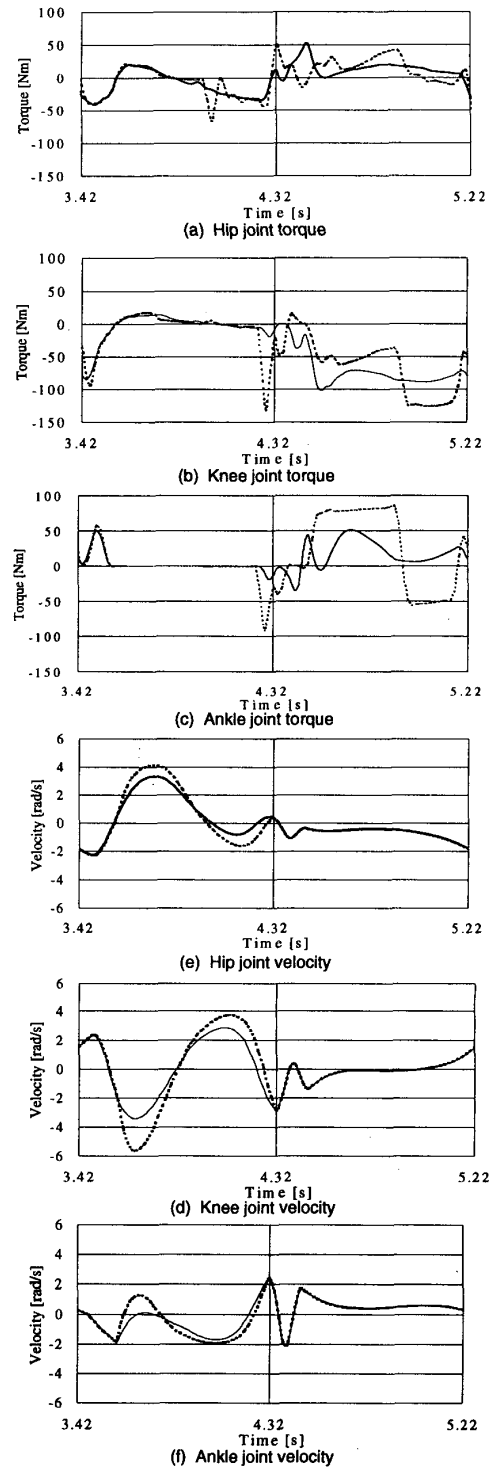
M_j is the solution of the following equations:

Fig. 7 Simulation results for different clearances
$q_b = -0.4\ [rad\ ]$, $q_f = 0.2\ [rad\ ]$, $L_{t0} = 0.25[m]$
$H_{hmax} = 0.83[m]$, $H_{hmax} = 0.82[m]$
- - - - : $H_{a0} = 0.23[m]$
———— : $H_{a0} = 0.16[m]$

(a) Hip joint torque

(b) Knee joint torque

(c) Ankle joint torque

(d) Hip joint velocity

(e) Knee joint velocity
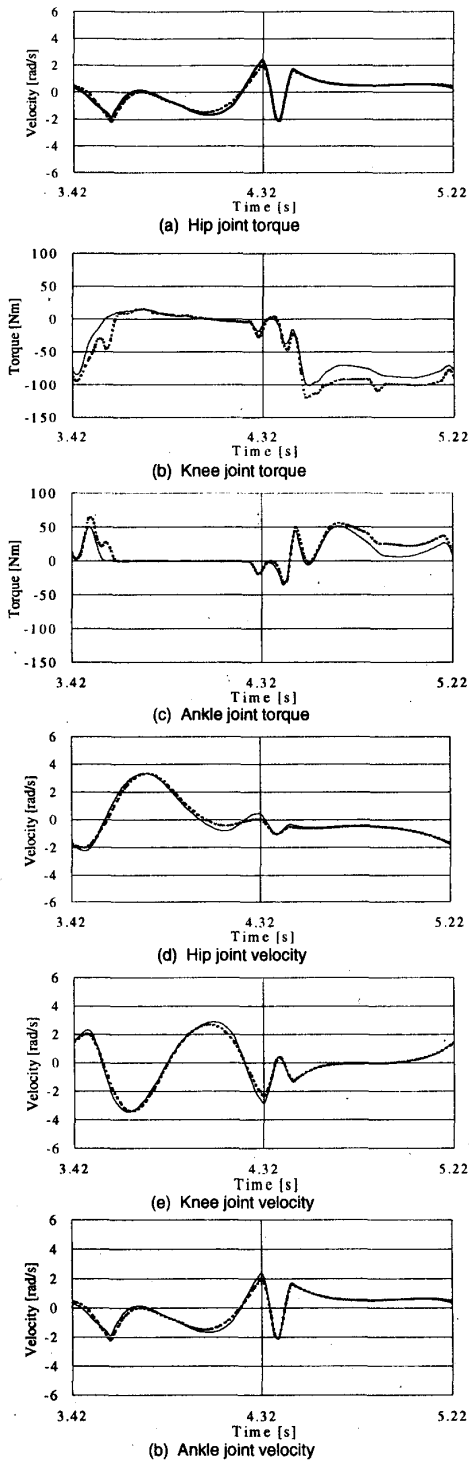
(b) Ankle joint velocity

Fig. 8 Simulation results for different hip height

$- - -$: $H_{hmax} = 0.80[m]$, $H_{hmin} = 0.79[m]$

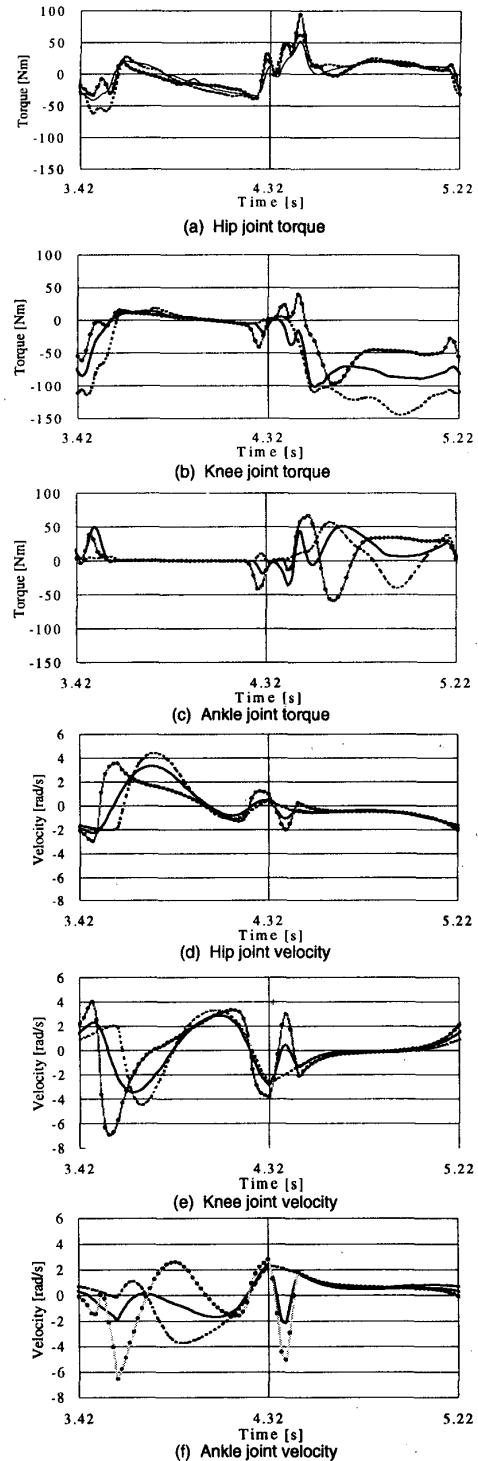——— : $H_{hmax} = 0.83[m]$, $H_{hmin} = 0.82[m]$

(a) Hip joint torque

(b) Knee joint torque

(c) Ankle joint torque

(d) Hip joint velocity

(e) Knee joint velocity

(f) Ankle joint velocity

Fig. 9 Simulation results for different foot slopes

$- - -$: $q_b = 0.0 \, [rad]$, $H_{hmax} = 0.77[m]$, $H_{hmin} = 0.76[m]$

——— : $q_b = -0.4 \, [rad]$, $H_{hmax} = 0.83[m]$, $H_{hmin} = 0.82[m]$

○-○-○-○-○ : $q_b = -1.0 \, [rad]$, $H_{hmax} = 0.87[m]$, $H_{hmin} = 0.86[m]$

$$\begin{cases} 2M_1 + b_1 M_2 = d_1 \\ \dfrac{h_{j-1}}{6} M_{j-1} + \dfrac{h_j + h_{j-1}}{3} M_j + \dfrac{h_j}{6} M_{j+1} \\ \qquad = \dfrac{f_{j+1} - f_j}{h_j} - \dfrac{f_j - f_{j-1}}{h_{j-1}} \quad (j = 2,3,\cdots,n-1) \\ a_n M_{n-1} + 2M_n = d_n \end{cases} \quad (11)$$

where,

$$\begin{cases} a_j = \dfrac{h_{j-1}}{h_j + h_{j-1}} \qquad b_j = 1 - a_j \qquad (j = 2,3,\cdots n-1) \\ c_j = \dfrac{f_{j+1} - f_j}{h_j} \qquad\qquad (j = 1,2,\cdots n-1) \\ d_j = \dfrac{6(c_j - c_{j-1})}{h_j + h_{j-1}} \qquad\quad (j = 2,3,\cdots n-1) \end{cases}$$

When initial constraint $S'(t_1) = 0$ and end constraint $S'(t_n) = 0$, the following equations are obtained:

$$\begin{cases} b_1 = a_n = 1 \\ d_1 = \dfrac{6(f_2 - f_1)}{h_1} \\ d_n = -\dfrac{6(f_n - f_{n-1})}{h_{n-1}} \end{cases} \quad (12)$$

Appendix B: ZMP Criterion

The ZMP is defined as the point on the ground about which the sum of all the moments of the active forces equals zero. If the ZMP is inside the contact polygon between the feet and the ground, the biped robot is stable. The contact polygon is called the stable region.

If the ZMP is near the center of the stable region, that is, when the stability margin (the minimum distance between the ZMP and the boundary of the stable region (Fig. 10)) is large, the biped robot will high stability. This stability margin can be regarded as an evaluation function of stability.
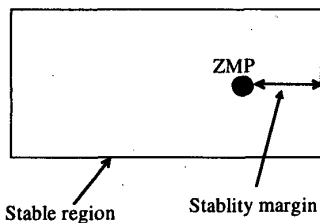

Fig. 10 Stable region and stability margin

References

[1] T. McGeer, "Passive Walking with Knees", Proc. IEEE Int. Conf. Robotics and Automation, pp. 1640-1645 (1990)

[2] P. H. Channon, S. H. Hopkins, and D. T. Phan, "Derivation of Optimal Walking Motions for a Biped Walking Robot", Robotica, Vol. 10, No. 2, pp. 165-172 (1992)

[3] M. Rostami and G. Bessonnet, "Impactless Sagittal Gait of a Biped Robot During the Single Support Phase", Proc. IEEE Int. Conf. Robotics and Automation, pp. 1385-1391 (1998)

[4] L. Roussel, C. Canudas-de-Wit, and A. Goswami, "Generation of Energy Optimal Complete Gait Cycles for Biped Robots", Proc.

IEEE Int. Conf. Robotics and Automation, pp. 2036-2041 (1998)

[5] C. Chevallereau, A. Formal'sky, and B. Perrin, "Low Energy Cost Reference Trajectories for a Biped Robot", Proc. IEEE Int. Conf. Robotics and Automation, pp. 1398-1404 (1998)

[6] F. M. Silva and J. A. T. Machado, "Towards Efficient Biped Robots", Proc. IEEE Int. Conf. Intelligent Robots and Systems, pp. 394-399 (1998)

[7] Y. F. Zheng and J. Shen, "Gait Synthesis for the SD-2 Biped Robot to Climb Sloping Surface," IEEE Trans. on Robotics and Automation, Vol. 6, No. 1, pp. 86-96 (1990)

[8] A. Takanishi, M. Ishida, Y. Yamazaki, and I. Kato, "The Realization of Dynamic Walking Robot WL-10RD", Proc. Int. Conf. Advanced Robotics, pp. 459-466 (1985)

[9] C.L. Shin, Y.Z. Li, S. Churng, T.T. Lee, and W.A. Cruver, "Trajectory Synthesis and Physical Admissibility for a Biped Robot During the Single-Support Phase", Proc. IEEE Int. Conf. Robotics and Automation, pp. 1646-1652 (1990)

[10] K. Hirai, M. Hirose, Y. Haikawa, and T. Takenaka, "The Development of Honda Humanoid Robot", Proc. IEEE Int. Conf. Robotics and Automation, pp. 1321-1326, (1998)

[11] Q. Huang, S. Kajita, N. Koyachi, K. Kaneko, K. Yokoi, H. Arai, K. Komoriya, and K. Tanie, "A High Stability, Smooth Walking Pattern for a Biped Robot", Proc. IEEE Int. Conf. Robotics and Automation, pp. 65-71, (1999)

[12] M. Vukobratovic and D. Juricic, "Contribution to the Synthesis of Biped Gait", IEEE Trans. on Bio-Medical Engineering, Vol. BME-16, No. 1, pp. 1-6 (1969)

[13] V. T. Inman, H.J. Ralston, and F. Todd, "Human Walking", Willams & Wilkins, Baltimore, 1981

[14] W. Braun and O. Fischer, "The Human Gait", Springer-Vorlag, Berlin Heidelberg, 1987

[15] K. Tsuchiya, "Introduction to Clinical Walking Analysis", Ishiya Pubilisher Inc. 1998 (in Japanese)

[16] D. W. Seward, A. Bradshaw, and F. Margrave, "The Anatomy of a Humanoid Robot", Robotica, Vol. 14, Part 4, pp. 437-443 (1996)

[17] D. G. Caldwell, N. Tsagarakis, D. Badihi, and G. A. Medrano-Cerda, "Pneumatic Muscle Actuator Technology a Light Weight Power System for a Humanoid Robot'", Proc. IEEE Int. Conf. Robotics and Automation, pp. 3053-3058, (1998)

[18] S. Kajita and K. Tani, "Adaptive Gait Control of a Biped Robot based on Realtime Sensing of the Ground Profile", Proc. IEEE Int. Conf. Robotics and Automation, pp. 570-577 (1996)

[19] S. M. Song and K.J. Waldron, "An Analytical Approach for Gait and its Application on Wave Gaits", Int. J. of Robotics Research, Vol. 6, No. 2, pp. 60-71, (1987)

[20] J.K., Hodgins and M.H. Raibert, "Adjusting Step Length for Rough Terrain Locomotion", IEEE Trans. on Robotics and Automation, Vol. 7, No. 3, pp. 289-298, (1991)

[21] Q. Huang, S. Sugano, and K. Tanie, "Stability Compensation of a Mobile Manipulator by Manipulator Motion: Feasibility and Planning", Proc. IEEE Int. Conf. Intelligent Robots and Systems, pp. 1285-1292 (1997)

[22] B.D. Bojanov, H.A. Hakopian and A.A. Sahakian, "Spline Function and Multivariate Interpolation", Kluwer Acadmedic Publishers, 1993

[23] D. W. Marhefka and D. E. Orin, "Simulation of Contact Using a Nonlinear Damping Model", Proc. IEEE Int. Conf. Robotics and Automation, pp. 1662-1668, (1996)

[24] O. Bruneau and F. B. Ouezdou, "Dynamic Walk Simulation of Various Bipeds via Ankle Trajectory", Proc. IEEE Int. Conf. Intelligent Robots and Systems, pp. 58-63 (1998)

[25] H. Han, T. Kim, and T. Park, "Tolerance Analysis of a Spur Gear Train", in Proc. 3rd DADS Korean User's Conf. , pp.61-81, 1987.

[26] J. Y. S. Luh, M. W. Walker, and R. P. C. Paul, "On-Line Computation Scheme for Mechanical Manipulators", Trans. of ASME, J. of Dynamic Systems, Measurement and Control, Vol.102, pp. 69-76 (1980)

[27] J. M. Hollerbach, "A Recursive Lagrangian Formulation of Manipulator Dynamics and a Comparative Study of Dynamics Formulation Complexity, IEEE Trans. Systems, Man, and Cybernetics, SMC-10-11, pp. 730-736, (1980)

[28] J. Furusho and A. Sano, "Sensor-Based Control of a Nine-Link Biped", Int. J. of Robotics Research, Vol. 9, No. 2, pp. 83-98, (1990)

[29] E.J. Haug, Computer-Aided Kinematics and Dynamics of Mechanical Systems, Basic Method, Allyn and Bacon, Inc. 1989.